

Superlattice-like $\text{Zn}_{15}\text{Sb}_{85}/\text{Ga}_{30}\text{Sb}_{70}$ thin films for low power and ultrafast phase change memory application

Rui Zhang¹, Yifeng Hu^{1,2,3} ✉, Qingqian Chou⁴, Tianshu Lai⁴, Xiaoqin Zhu¹

¹School of Mathematics and Physics, Jiangsu University of Technology, Changzhou 213000, People's Republic of China

²State Key Laboratory of Silicon Materials, Zhejiang University, Hangzhou 310027, People's Republic of China

³Key Laboratory of Microelectronic Devices & Integrated Technology, Institute of Microelectronics, Chinese Academy of Sciences, Beijing 100029, People's Republic of China

⁴State-Key Laboratory of Optoelectronic Materials and Technology, School of Physics, Sun Yat-Sen University, Guangzhou 510275, People's Republic of China

✉ E-mail: hyf@jsut.edu.cn

Published in Micro & Nano Letters; Received on 18th August 2018; Revised on 14th November 2018; Accepted on 5th December 2018

In this study, the amorphous-to-crystalline transitions of superlattice-like (SLL) $\text{Zn}_{15}\text{Sb}_{85}/\text{Ga}_{30}\text{Sb}_{70}$ thin films were investigated by in situ film resistance measurement. The thermal stability, resistance and band gap of the SLL $\text{Zn}_{15}\text{Sb}_{85}/\text{Ga}_{30}\text{Sb}_{70}$ thin film perform well. The data retention temperature for 10 years increases from 177°C of $[\text{Zn}_{15}\text{Sb}_{85}/\text{Ga}_{30}\text{Sb}_{70}]_3$ to 220°C of $[\text{Zn}_{15}\text{Sb}_{85}/\text{Ga}_{30}\text{Sb}_{70}]_8$. The X-ray diffraction patterns show the presence of a large amount of Sb phase in the $\text{Zn}_{15}\text{Sb}_{85}/\text{Ga}_{30}\text{Sb}_{70}$ thin films, which causes a rapid phase transition. The surface morphology is observed by atomic force microscopy, which indicates that the thickness of $\text{Ga}_{30}\text{Sb}_{70}$ in the SLL thin films can affect the grain size and inhibit the crystallisation process. For the $\text{Zn}_{15}\text{Sb}_{85}/\text{Ga}_{30}\text{Sb}_{70}$ thin films, an ultra-short switching time of around 2 ns is achieved. These results indicate that the SLL $\text{Zn}_{15}\text{Sb}_{85}/\text{Ga}_{30}\text{Sb}_{70}$ thin films have a promised application in phase change memory.

1. Introduction: In recent years, the conventional flash memory is facing a performance bottleneck due to its physical limit, such as limited data transfer rate and scaling down of cell size. In this study, many new non-volatile memories have been proposed and extensively studied [1]. Phase-change memory (PCM) is considered as one of the most promising candidates for future non-volatile data storage due to its advantages of fast operation speed, high capacity, good reliability, low power and so on [2]. Especially, PCM has shown its tremendous potential as synaptic elements in the artificial neural network [3]. The working principle of PCM is to distinguish two resistance states, marked with a high resistance state (order state '0') and a low resistance state (disorder state '1') [4]. Also, data storage is achieved by a reversible phase change between order and disorder states caused by electrical pulses. Due to the significant difference in resistivity between the two states, PCM devices can be used as practical high performance memory components [5].

Phase change materials have a great impact on the properties of PCM, so there is a high demand for the development of new phase change materials [6]. The most widely used phase change materials are chalcogenide, of which $\text{Ge}_2\text{Sb}_2\text{Te}_5$ (GST) has been extensively studied and widely used in commercial DVD-RAM for a long time with its excellent performance [7]. However, some aspects limit its application in PCM, such as the low activation energy (2.24 eV for the phase change from the crystal to rock salt structure) [8, 9], the great density change (6.8% from amorphous to NaCl-type crystal state) [10], high RESET current (>1 mA) [11] and the long crystallisation time (~ 100 ns) [11]. It is reported that Sb-rich phase change material has fast switching speed due to its growth-dominated crystallisation mechanism, such as Ge-Sb [12], Sn-Sb [13] and Cu-Sb-Te [14]. At the same time, Te element is harmful to semiconductor technology due to its volatilisation [15]. Thus, the Te-free and Sb-rich thin films have been considered as the promising candidate for replacing GST. The superlattice-like (SLL) phase change films exhibit faster operating speeds and lower programming currents due to much lower thermal conductivity than monolayer films [16]. Moreover, the SLL thin films can combine the phase change performance of different composite layers to obtain

an excellent comprehensive property [17]. In this work, two thin films of $\text{Zn}_{15}\text{Sb}_{85}$ (ZS) and $\text{Ga}_{40}\text{Sb}_{60}$ (GS) are used to prepare SLL ZS/GS thin films. The potential application in PCM can be evaluated by assessing the thermal and electrical properties of the thin films.

2. Experimental methods: Before sputtering the films, Si/SiO₂ substrates were washed with distilled water after cleaning in ethanol. Then, Si/SiO₂ substrates were glued onto sample plates with double-faced adhesive. The SLL thin films were deposited on a 0.5 mm thick silicon oxide (100) wafer at room temperature using a radio frequency (RF) magnetron sputtering system (JGP 450). Prior to the growth of SLL ZS/GS thin films, the deposition rates of ZnSb and GaSb monolayers were predetermined which are measured by an Alpha-Step 500 analyser (Tencor instrument). The thickness of each individual layer can be designed by controlling the deposition time. The total thickness of the films was set to be about 50 nm. The purity of ZS and GS targets is 99.999%. The SLL structure was obtained by alternately sputtering ZS and GS targets. The vacuum of the RF magnetron sputtering system before sputtering was 3×10^{-4} Pa. The deposition process was carried out at a flow rate of 30 sccm and an RF power of 30 W in an Ar atmosphere at a pressure of 0.4 Pa. In order to ensure uniformity of deposition, the substrate automatically rotated at 20 rpm. The working temperature is room temperature.

The dependence of the sheet resistance on the temperature ($R-T$) of the SLL thin films was measured by a Pt-100 thermocouple located at a heating stage controlled by a TP 94 temperature controller (Linkam Scientific Instruments Ltd, Surrey, UK). The thermal stability of amorphous thin films was evaluated by isothermal time-dependent resistance measurements. A near infrared spectroscopy was used to measure the optical band gap. The range of measurement wavelengths was set from 400 to 2500 nm. The phase structure was investigated by X-ray diffraction (XRD) operated at 40 kV and 40 mA using a Cu-K α source with the 2θ degrees range from 20° to 60°. The atomic force microscopy (AFM) was used to observe the surface morphology of thin films.

The real-time reflectivity measurement was tested by a picosecond laser pump-probe system. The light source used for irradiating the samples was a frequency-doubled model-locked neodymium yttrium aluminium garnet laser with the operating wave-length of 532 nm and pulse duration of 30 ps.

3. Results and discussion: The R–T curves of monolayer layer ZS and GS are shown in Fig. 1a. Fig. 1b shows the R–T curves of SLL ZS/GS thin films at a constant heating rate of 20°C/min. From Figs. 1a and b, it can be found that the resistance decreases slowly with the temperature elevating from the start. Then the resistance drops rapidly to a low and stable value, indicating the transition of amorphous to crystalline state. The temperature at which the great decline of resistance happens is defined as the crystallisation temperature (T_c). As shown in Fig. 1b, the T_c of ZS (50 nm) and GS (50 nm) is ~145 and 355°C, respectively. In general, the phase change speed is inverse correlation with the thermal stability. Fig. 1a illustrates that ZS has a fast crystallisation rate but low thermal stability. In contrast to ZS, GS has better thermal stability but lower speed. The conventional doping method often sacrifices parts of the speed performance for improving thermal stability. It cannot make the best of both worlds. Fig. 1b shows the T_c of [ZS2/GS8]₅, [ZS3/GS7]₅, [ZS5/GS5]₅, [ZS6/GS4]₅ and [ZS7/GS3]₅ (the numbers such as 2 and 8 in [ZS2/GS8] are the thicknesses of the ZS thin films and the GS thin films, respectively). At the same time, 5 in [ZS2/GS8]₅ indicates the number of cycles of sputtering) thin films are ~177, ~185, ~190, ~205 and

~220°C, respectively. The thermal stability of the metastable amorphous state depends a lot on the crystallisation temperature. It is obvious to see that as the thickness of the GS layer increases, the thermal stability becomes better. The amorphous resistances of [ZS2/GS8]₅, [ZS3/GS7]₅, [ZS5/GS5]₅, [ZS6/GS4]₅ and [ZS7/GS3]₅ are 4.5×10^5 , 6.1×10^5 , 1.0×10^6 , 2×10^6 and $3.1 \times 10^6 \Omega$, respectively.

The crystallisation resistance also increases from $7 \times 10^2 \Omega$ of [ZS6/GS4]₅ to $2 \times 10^3 \Omega$ of [ZS2/GS8]. According to the joule heat $Q = I^2 \times R \times t$, a higher crystallisation resistance can improve the heating efficiency and decrease the power consumption [11]. Therefore, we can conclude that [ZS2/GS8]₅, [ZS3/GS7]₅, [ZS5/GS5]₅, [ZS6/GS4]₅ and [ZS7/GS3]₅ thin films have lower RESET power consumption than ZS. Also, the resistance difference for ZS/GS thin films between amorphous and crystalline state is more than one order of magnitude, which can meet the application for PCM.

The band gap energy (E_g) can be determined by extrapolating the absorption edge onto the energy axis, as shown in Fig. 1c where in the conversion of the reflectivity to absorbance data is obtained by the Kubelka–Munk function (K–M) [12]

$$K/S = (1 - R)(1 - R)^2 / (2R), \quad (1)$$

where R is the reflectivity, K is the absorption coefficient, and S is the scattering coefficient. Fig. 1c shows that the E_g increases

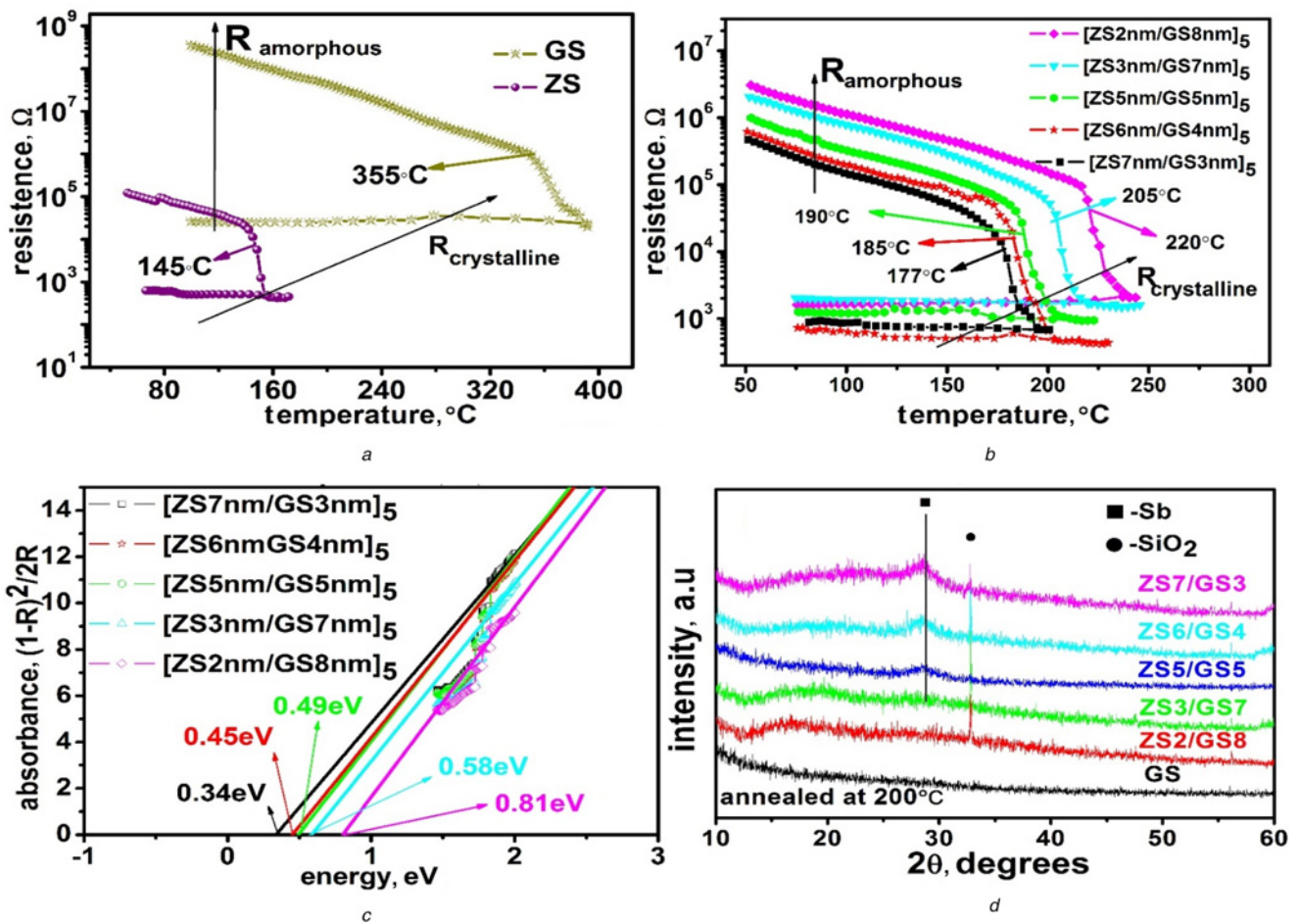


Fig. 1 Properties of thin films including resistance, energy bandgap and XRD phase structure

a R–T curves of the monolayer ZS and GS thin films at a heating rate of 20°C/min

b R–T curves of the SLL [ZS_x/GS(10–x)]₅ thin films at the heating rate of 20°C/min

c Kubelka–Munk function of amorphous of the SLL [ZS_x/GS(10–x)]₅ thin films

d XRD patterns of SLL [ZS_x/GS(10–x)]₅ thin films and monolayer GS(50 nm) thin films annealed at 200°C for 25 min in an Ar atmosphere

gradually with the increase of the thickness of the GS layer. The E_g for [ZS7/GS]₅, [ZS6/GS4]₅, [ZS5/GS]₅, [ZS3/GS7]₅ and [ZS2/GS8]₅ are 0.34, 0.45, 0.49, 0.58, and 0.81 eV, respectively. The difference for E_g is related to the carrier concentration. Since the carrier density inside the semiconductors is proportional to $\exp(-E_g/2KT)$ [13]. A broad band gap will increase the obstacle of carrier transition, leading to the reduction of carriers. After more GS is added, it plays a major role in the increase in resistivity of the films. This finding supports the conclusions of resistance curves in Fig. 1a.

Fig. 1d shows the XRD pattern of SLL ZS/GS thin films annealed at 200°C for 25 min in an Ar gas. For [ZS2/GS8]₅ and [ZS3/GS7]₅, no obvious diffraction peaks are observed, indicating that the SLL thin films are amorphous at low-annealing

temperature. By contrast, the peaks (012) belonging to the Sb phase appear in annealed [ZS7/GS3]₅, [ZS6/GS4]₅ and [ZS5/GS5]₅ thin films. Also, the intensity of Sb peak increase with the thickness of ZS interval layer. The existence of a great deal of Sb phases conduces to accelerate the phase change by forming weak Sb-Sb bonds. The results of XRD demonstrate that the thermal stability of the SLL ZS/GS thin films has been improved by adding the GS layer to inhibit the crystallisation.

Isothermal crystallisation tests are carried out to further evaluate the thermal stability of the phase change films. Figs. 2a–e show the normalised resistance as a function of the annealing time for the SLL ZS/GS thin films at different temperatures. The time is defined as the failure time when the resistance dropped to half of its initial value.

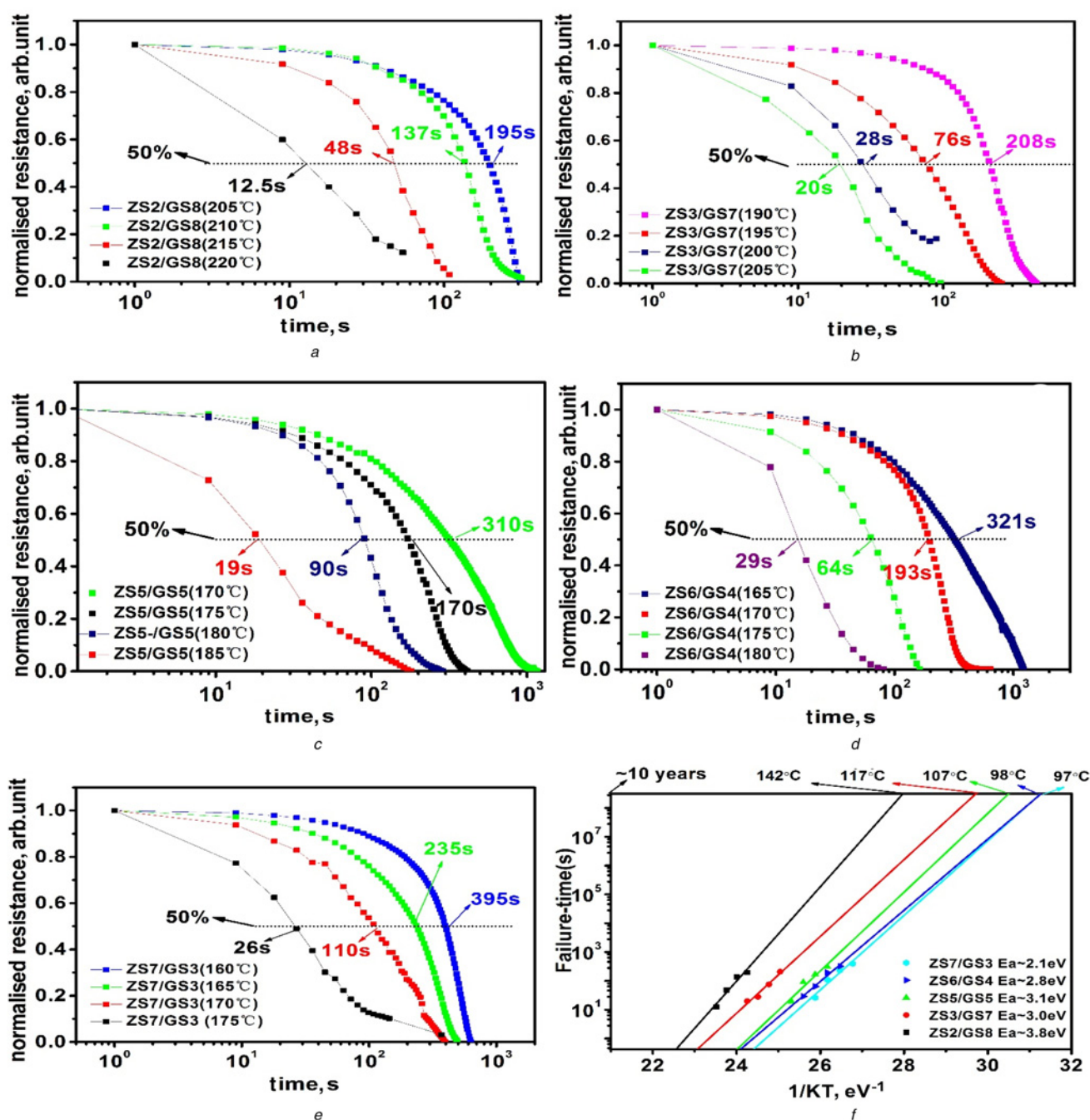


Fig. 2 Curves of thermal stability and data retention

a–e Normalised resistance of the SLL [ZS_x/GaSb(10–x)] thin film as a function of annealing time at various temperatures
f Plot of failure time versus reciprocal temperature, showing the data retention temperature for 10 years and Kissinger plots for E_a

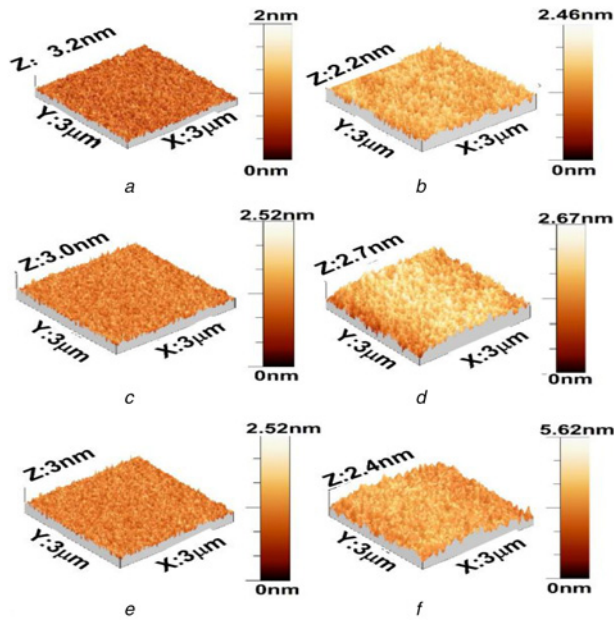


Fig. 3 AFM topographic images of *a, c, e* As-deposited the SLL $[ZS_x/GaSb(10-x)]_5$ ($x=5, 6, 7$) thin films *b, d, f* Annealed $[ZS_x/GS(10-x)]_5$ ($x=5, 6, 7$) thin films at 280°C

The isothermal crystallisation process can be roughly divided into four stages, including incubation, nucleation, grains growth and grains coarse. Figs. 2a–3e show the incubation period, in which the phase transition is time dependent [18]. A lower isothermal annealing temperature will result in a longer incubation time. For SLL $[ZS2/GS8]_5$ thin film, the annealing temperature is selected from 205 to 220°C, so the change begins from an amorphous state. As shown in Fig. 3a, the $[ZS2/GS8]$ thin film has a failure time of 12.5 s at 220°C. However, as the annealing temperature dropped to 215, 210 and 205°C, respectively, the failure time increases to 48, 137 and 195 s. Similarly, isothermal annealing experiments for the other SLL ZS/GS thin films are also described in Figs. 3b–e. Fig. 3b shows the failure time of $[ZS3/GS7]_5$ at 205, 200, 195 and 190°C is 20, 28, 760 and 208 s, respectively. The plot of logarithm failure time versus $1/k_b T$, exhibited in Fig. 2f, fits a linear Arrhenius relationship because of its thermal activation nature. The linear relationship is described as follows [14]:

$$t = \tau_0 \exp[E_c / (k_b \times T)], \quad (2)$$

where t , τ_0 , k_b , and T are failure time, a pre-exponential factor depending on the thin film's properties, Boltzmann constant and absolute temperature, respectively [15]. The 10-year data retention temperature (T_{10}) is obtained by extending the fitted lines, which can be used to estimate the reliability of the phase change thin films [19]. The T_{10} for $[ZS_x/GS(10-x)]_5$ ($x=7, 6, 5, 3, 2$) are 97, 98, 107, 117 and 142°C individually. Obviously, as the thickness of the GS layer gradually increases, the T_{10} of SLL ZS/GS thin films is getting larger and larger, which means that the thermal stability has been enhanced. By comparing the data retention of GST (85°C), it can be found that the all SLL ZS/GS thin films have better data reliability than GST.

At the same time, the activation energy (E_a) of each thin film can be acquired from the slope of the straight line in the corresponding Kissinger plots [16] with the results of $[ZS2/GS8]_5$: 2.1 eV, $[ZS3/GS7]_5$: 2.8 eV, $[ZS5/GS5]_5$: 3.1 eV, $[ZS6/GS4]_5$: 3.0 eV, $[ZS7/GS3]_5$: 3.8 eV, respectively. It shows that E_a also increases as the thickness of the GS layer. The larger E_a means that it is more difficult to crystallise, resulting in better thermal stability.

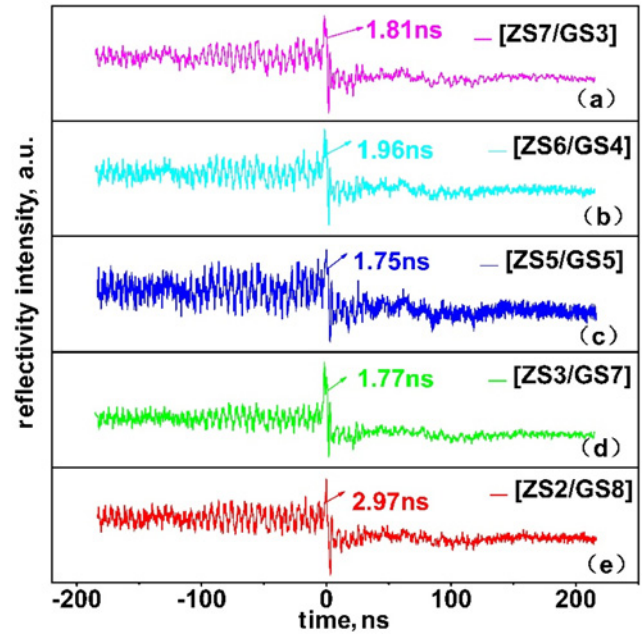


Fig. 4 Reflectivity evolutions in the amorphisation process for $[ZS_x/GS(10-x)]_5$ ($x=7, 6, 5, 3, 2$) thin films

The surface roughness of the phase change thin films affects the quality of the interface between the electrode and phase change layer. The surface of as-deposited and annealed SLL ZS/GS thin films is observed by using AFM. Figs. 3a–f exhibit the AFM images of $[ZS_x/GS(10-x)]_5$ ($x=5, 6, 7$) thin films. The root-mean-square (RMS) surface roughness was 0.2474, 0.2861 and 0.2913 nm for as-deposited $[As/GS(10-x)]_5$ ($x=5, 6, 7$), respectively, which means the surface is smooth. After annealing at 280°C for 35 min, the RMS of $[ZS_x/GS(10-x)]_5$ ($x=5, 6, 7$) thin films increases to 0.2665, 0.3378 and 0.5116 nm. While the surface of the SLL thin films becomes slightly rougher after crystallisation. Overall the RMS is small, which can ensure the durability of the PCM devices and improve the fatigue performance of the PCM. The phase change speed of thin films is a crucial feature because it has a great influence on the switching performance of PCM devices. During the phase change, the optical reflectivity also has a great change except for the resistivity. The abrupt decrease of reflectivity, shown in Fig. 4, is regarded as the crystalline-to-amorphous phase transition. The crystalline SLL thin films exhibit high reflectivity and the amorphous SLL thin films exhibit low reflectivity. After the irradiation of pulse laser, the heat generated by the pulse triggers the reset process of the SLL thin films, reducing the reflectivity of the thin films. The results reveal that the time for SLL $[ZS_x/GS(10-x)]_5$ ($x=7, 6, 5, 3, 2$) thin films during the amorphisation process is 1.81, 1.96, 1.75, 1.77 and 1.97 ns, respectively. It is reported that the GST thin film need about 39 ns to realise the same switching. This demonstrated that the phase transition rate of $[ZS_x/GS(10-x)]_5$ ($x=7, 6, 5, 3, 2$) is faster than GST and a lower power consumption could be achieved if the PCM device is based on the SLL $[ZS_x/GS(10-x)]_5$ ($x=7, 6, 5, 3, 2$) thin films.

The Sb-rich ingredient as well as low-thermal conductivity of the SLL structure work together to endow SLL ZS/GS thin films with good thermal stability and ultrafast phase change speed.

4. Conclusions: In this work, SLL ZS/GS thin films were proved to have improved thermal stability, including crystallisation temperature, data retention for ten years and activation energy ($[ZS2/GS8]_5$: $T_c \sim 177^\circ\text{C}$, $T_{10} \sim 97^\circ\text{C}$, $E_a \sim 2.1$ eV; $[ZS3/GS7]_5$: $T_c \sim 185^\circ\text{C}$, $T_{10} \sim 98^\circ\text{C}$, $E_a \sim 2.8$ eV; $[ZS5/GS5]_5$: $T_c \sim 190^\circ\text{C}$,

$T_{10} \sim 107^\circ\text{C}$, $E_a \sim 3.1$ eV; [ZS6/GS4]₅: $T_c \sim 205^\circ\text{C}$, $T_{10} \sim 117^\circ\text{C}$, $E_a \sim 3.0$ eV and [ZS7/GS3]₅: $T_c \sim 220^\circ\text{C}$, $T_{10} \sim 142^\circ\text{C}$, $E_a \sim 3.8$ eV. The band gap is gradually broadened as the thickness of the GS layer in the SLL ZS/GS thin films increase, from [ZS7/GS3]₅: 0.34 eV to [ZS2/GS8]₅: 0.81 eV. For the crystallisation [ZS_x/GS(10 - x)] ($x=3$) thin films, a smaller surface roughness is observed, which ensure the reliability of the PCM device. The ultrafast phase transition speed of [ZS_x/GS(10 - x)]₅ thin film below 3.0 ns is achieved which are much faster than GST (39 ns). The results show that the SLL ZS/GS thin films have good thermal stability and fast phase transition speed, which are suitable for PCM applications.

5. Acknowledgments: This work was supported by the National Natural Science Foundation of China (grant no. 11774438) and the Natural Science Foundation of Jiangsu Province (grant no. BK20151172) and sponsored by Qing Lan Project and Postgraduate Research and Practice Innovation Program of Jiangsu Province (grant no. SJCX18_1062) and the Opening Project of State Key Laboratory of Silicon Materials (grant no. SKL2017-04) and the Opening Project of Key Laboratory of Microelectronic Devices & Integrated Technology, Institute of Microelectronics, Chinese Academy of Sciences and Postgraduate Research.

6 References

- [1] Zou H., Hu Y.F., Zhu X.Q., *ET AL.*: 'Simultaneously high thermal stability and ultra-fast phase change speed based on samarium-doped antimony thin films', *RSC Adv.*, 2017, **7**, (49), pp. 31110–31114
- [2] Wu W.H., Chen S.Y., Zhai J.W., *ET AL.*: 'Ti_xSb_{100-x} thin films as candidates for phase-change memory application', *Appl. Phys. Lett.*, 2017, **110**, (18), p. 181906
- [3] Ren K., Li R.H., Chen X., *ET AL.*: 'Controllable SET process in O–Ti–Sb–Te based phase change memory for synaptic application', *Appl. Phys. Lett.*, 2018, **112**, p. 073106
- [4] Wang C.Z., Zhai J.W., Bai S.Y., *ET AL.*: 'Phase transition behaviors and thermal conductivity measurements of nitrogen-doped Sb₂Te₃ thin films', *Mater. Lett.*, 2010, **64**, (21), pp. 2314–2316
- [5] Peng C., Rao F., Wu L.C., *ET AL.*: 'Homogeneous phase W-Ge-Te material with improved overall phase-change properties for future nonvolatile memory', *Acta Mater.*, 2014, **74**, pp. 49–57
- [6] Ren K., Rao F., Song Z.T., *ET AL.*: 'Phase change material W_{0.04}(Sb₄Te)_{0.96} for application in high-speed phase change memory', *J. Alloy. Compd.*, 2014, **594**, pp. 82–86
- [7] Huang Y.J., Tsai M.C., Wang C.H., *ET AL.*: 'Characterizations and thermal stability improvement of phase-change memory device containing Ce-doped GeSbTe films', *Thin Solid Films*, 2012, **520**, (9), pp. 3692–3696
- [8] Zhu X.Q., Hu Y.F., Zou H., *ET AL.*: 'Si/Sb superlattice-like thin films for ultrafast and low power phase change memory application', *Scr. Mater.*, 2016, **121**, pp. 66–69
- [9] Zhang W., Wu D.Y., Hu Y.F., *ET AL.*: 'Effect of thickness on crystallization behavior in GeSb₉ phase change films', *J. Mater. Sci., Mater. Electron.*, 2016, **27**, (12), pp. 13148–13153
- [10] Sun X.X., Ehrhardt M., Lotnyk A., *ET AL.*: 'Crystallization of Ge₂Sb₂Te₅ thin films by nano- and femtosecond single laser pulse irradiation', *Sci. Rep.*, 2016, **6**, p. 28246
- [11] Zheng L., Zhu X.Q., Zhai L.J., *ET AL.*: 'Interface effect and stress effect on Ge₂Sb₂Te₅/Sb superlattice-like thin films', *EUR Phys. J. Appl. Phys.*, 2017, **77**, (3), p. 30102 (4 pp.)
- [12] Kim Y.T., Kim Y.H.: 'Microstructural failure in Ge₂Sb₂Te₅ phase change memory cell', *Phys. Status Solidi B*, 2014, **251**, (2), pp. 435–438
- [13] He Z.F., Wu P.Z., Liu R.R., *ET AL.*: 'Superlattice-like SnSb₄/Ge thin films for ultra-high speed phase change memory applications', *CrystEngComm*, 2016, **18**, (7), pp. 1230–1234
- [14] Lu Y.G., Song S.N., Song Z.T., *ET AL.*: 'Superlattice-like electrode for low-power phase-change random access memory', *Appl. Phys. Lett.*, 2012, **101**, (11), p. 113104
- [15] Dai M., Xu L., Liu D., *ET AL.*: 'Fabrication and phase transition of long-range-ordered, high-density GST nanoparticle arrays', *Nanotechnology*, 2008, **19**, (50), p. 505304
- [16] Hu Y.F., Zhu X.Q., Zou H., *ET AL.*: 'Nanosecond switching in superlattice-like GeTe/Sb thin film for high speed and low power phase change memory application', *ECS J. Solid State Sci.*, 2017, **6**, (1), pp. 45–48
- [17] Li L., Song S.N., Zhang Z.H., *ET AL.*: 'Superlattice-like film for high data retention and high speed phase change random access memory', *Solid. State Electron.*, 2016, **120**, pp. 52–55
- [18] Lu Y., Hu Y.F., Yuan L., *ET AL.*: 'SnSb₄/SiO₂ multilayered thin films for phase change memory applications', *J. Non-Cryst. Solids.*, 2016, **432**, Part B, pp. 505–509
- [19] Rao F., Song Z.T., Ren K., *ET AL.*: 'Sn₁₂Sb₈₈ material for phase change memory', *Appl. Phys. Lett.*, 2009, **95**, (3), p. 03210